CONF-970517--

LA-UR- 97-2196

Approved for public release; distribution is unlimited.

Title:

MODELING OF POLYMER ELECTROLYTE FUEL CELL PERFORMANCE WITH REFORMATE FUEL FEED STREAMS

Author(s):

Thomas E. Springer - MST-11
Thomas A. Zawodzinski - MST-11
Shimshon Gottesfeld - MST-11

Submitted to:

Proceedings of the Symposium on Electrode Processes for Energy Conversion and Storage IV. To be published by the Electrochemical Society

MASTER

19980407 005

DISTRIBUTION OF THIS DOCUMENT IS UNLIMITED

Los Alamos
NATIONAL LABORATORY

Modeling of Polymer Electrolyte Fuel Cell Performance with Reformate Fuel Feed Streams

T. Springer, T. Zawodzinski and S. Gottesfeld

Los Alamos National Laboratory
Los Alamos, NM 87545

Introduction

Carbon monoxide poisoning of polymer electrolyte fuel cell anodes is a key problem to be overcome when operating on reformed fuels. CO adsorbs on the precious metal surface leading to substantial performance losses. Much recent work has explored this problem, using various Pt alloys in attempts to overcome the performance loss.

In their studies of hydrogen oxidation on Pt and Pt alloy (Pt/Sn, Pt/Ru) electrodes exposed to H_2/CO mixtures, Gasteiger et al. (1, 2) showed that a small oxidation current is observed before the onset of CO oxidative stripping (ca. 0.4 V) on Pt/Ru. However, these workers concluded that the observed current was 'too low to be of practical value.' Nonetheless, we and others (3-5) have found experimentally that it is indeed possible to run a PEFC with a Pt/Ru anode in the presence of CO with little loss.

In this work, we describe our recent work aimed at modeling the performance of a PEFC exposed to CO at the anode. The philosophy behind this work is to treat the anode loss strictly as a problem of electrode kinetics, ignoring mass transfer effects, and looking to see if the overall morphology of the calculated polarization curves catches the general features of polarization curves observed for PEFCs operating in the presence of CO. This approach is reasonable in the absence of any 'sink' for CO in the catalyst layer which could couple to mass transfer effects.

Results and Discussion

We present here a relatively uncomplicated model of CO effects on a PEFC hydrogen anode. We assume the dry anode reactant gas consists of almost pure H_2 with

We present here a relatively uncomplicated model of CO effects on a PEFC hydrogen anode. We assume the dry anode reactant gas consists of almost pure H_2 with less than 1000 parts per million (ppm) of CO, and is then fully saturated with water vapor at the cell temperature. We can then be assured that the hydrogen concentration will always remain fixed by the saturation conditions, so effects of mass transport losses from interdiffusion of gases through the gas diffusion backing can be ignored. We also assume that the catalyst layer ionic resistance will be low enough to ignore any potential change across the catalyst layer. The model will concentrate primarily on the kinetic competition between hydrogen and carbon monoxide for sites on the Pt/ Ru catalyst to determine the local current density from hydrogen oxidation and, secondarily, on the effect of CO diffusion through the catalyst layer on the total current density.

We assume the interfacial kinetics is determined by the four processes that are expressed in Eq. 1 to 4.

$$\mathrm{CO + Pt} \underset{b_{fc}k_{fc}}{\overset{k_{fc}}{\rightleftarrows}} \mathrm{(Pt\text{-}CO)} \qquad [1]$$

$$\mathrm{H_2 + 2Pt} \underset{b_{fh}k_{fh}}{\overset{k_{fh}}{\rightleftarrows}} \mathrm{2(Pt-H)} \qquad [2]$$

$$\mathrm{(Pt\text{-}H)} \xrightarrow{k_{eh}} \mathrm{H^+} + e^- + \mathrm{Pt} \qquad [3]$$

$$\mathrm{(H_2O + (Pt\text{-}CO)} \xrightarrow{k_{ec}} \mathrm{Pt + CO_2 + H^+} + e^- \qquad [4]$$

The first two equations represent adsorption of CO and dissociative chemisorption of H_2. All the forward rate constants k_i are expressed in A/cm^2 (geometric). The desorption rates are implicit in b_{fh} and b_{fc}, the ratio of backward to forward rate constants. Most of the electrical current density is produced by the third process (Eq. 3), the electrochemical oxidation of the adsorbed hydrogen. At higher overpotentials the fourth process (Eq. 4), the electrochemical oxidation of CO to CO_2 begins to provide more hydrogen sites to increase the current density.

Equations 5 and 6 represent the steady balance of equivalent current densities of adsorption, desorption, and charge transfer fluxes of carbon monoxide and hydrogen species that will determine θ_{co}, the fraction of catalyst sites with adsorbed CO, and θ_h, the fraction with adsorbed H. The quantity ρ represents the molar areal density of catalyst sites times the Faraday constant.

$$\rho\dot{\theta}_{co} = k_{fc}P_{co}\left(1-\theta_{co}-\theta_h\right) - b_{fc}k_{fc}\theta_{co} - k_{ec}\theta_{co}e^{\frac{\eta}{b_c}} = 0 \qquad [5]$$

$$\rho\dot{\theta}_h = \mathrm{k}_{\mathrm{fh}}P_h\left(1-\theta_{co}-\theta_h\right)^2 - b_{fh}\,\mathrm{k}_{\mathrm{fh}}\theta_h^2 - 2\theta_h k_{eh}\sinh\left(\frac{\eta}{b_h}\right) = 0 \qquad [6]$$

$$j_h = 2k_{eh}\theta_h\sinh\left(\frac{\eta}{b_h}\right),\ j_{co} = k_{ec}\theta_{co}e^{\frac{\eta}{b_c}} \qquad [7]$$

Expressions for the potential dependence of the current densities for hydrogen and CO oxidation, j_h and j_{co}, are given in Eq. 7 and assume a transfer coefficient of 0.5.

This system of equations was solved analytically by Mathematica (Wolfram). Expressions for j_h and j_{co} (independent of θ_h and θ_{co}) are given in Eq. 8 and 9:

$$s_1 = k_{eh}\sinh\left(\frac{\eta}{b_h}\right)$$

$$a_1 = e^{\frac{\eta}{b_c}}k_{ec} + k_{fc}\left(b_{fc}+P_{co}\right),\ a_2 = \left(e^{\frac{\eta}{b_c}}k_{ec} + b_{fc}k_{fc}\right)^2,\ a_3 = b_{fh}\,\mathrm{k}_{\mathrm{fh}} + 2s_1$$

$$j_h = \frac{2s_1\left(a_1\sqrt{a_2a_3k_{fh}P_h + a_1^2s_1^2} - a_1^2s_1 - a_2k_{fh}P_h\right)}{k_{fh}\left(b_{fh}a_1^2 - a_2P_h\right)} \qquad [8]$$

$$j_{co} = \frac{e^{\frac{\eta}{b_c}}k_{ec}k_{fc}P_{co}\left(a_1b_{fh}k_{fh} + a_1s_1 - \sqrt{a_2b_{fh}k_{fh}^2P_h + 2a_2k_{fh}P_hs_1 + a_1^2s_1^2}\right)}{k_{fh}\left(b_{fh}a_1^2 - a_2P_h\right)} \qquad [9]$$

Applications of Equations 8 and 9: We first consider a base case using estimates of electrochemical and adsorption rate constants obtained typical of the literature values.

Our goal is to determine whether at least qualitatively correct behavior of anode polarization in the presence of CO can be obtained from this simple kinetic model. Table I lists a set of parameters that approximates the observed anode overpotential on a Pt catalyst as a function of current density for various CO concentrations at 80°C.

Figure 1 shows a set of anode overpotentials as a function of current density for the conditions of Table I. This approximately matches a set of measured data on Pt at 80°C. For the purpose of visual comparison to the more common form of data in the literature, Figure 2 shows cell polarization for the same set of conditions, obtained by subtracting the anode polarization from using a typical cell current/voltage curve for H_2/Air. The polarization curves thus obtained exhibit several of the characteristic features of polarization curves experimentally obtained for Pt or Pt-Ru-based cells exposed to CO in the anode feed. In each case shown in Figures 1 and 2, there is a region of low current density for which little loss is observed, followed by a region of steeper decline in the polarization curve and finally leveling off to a constant level of polarization loss. The region of little polarization loss is dependent on the CO level. The current density in that region represents the hydrogen oxidation current on the few uncovered catalyst sites available. The availability of such sites is of course related tothe equilibrium coverage of CO on the catalyst.

Effect of electrochemical stripping of CO

To develop further insight into the factors allowing hydrogen oxidation in thepresence of CO, we proceed to explore the effects of perturbations of the base case parameters. Figure 3 shows the effect of varying k_{ec}, the rate constant for electrochemical stripping of CO. We see that in creasing the rate of electrochemical CO stripping does not effect the extremely low current range of the curve (below 50 mA/cm^2). However, this behavior is a reflection of our assumptions concerning equilibrium coverage of CO on the catalyst surface. It also is a reflection of he extremely low rates of electrochemical stripping used in Figure 3.

If we evaluate Eq. 8 when k_{ec} is 0 and η is large we get a limiting current density j_{ll} which indicates the location of the steep inflections in Fig. 1 and which is indeed a limiting current if k_{ec} were really zero as we show in Fig. 4. Figure 4 shows the dependence of the limiting current obtained in the absence of CO electrostripping for various CO concentrations. Note that the limiting currents of equation 4 correspond to the inflections in Fig. 1. An expression for the limiting curent density, j_{ll}, is shown in Eq. 10,

$$j_{ll} = \left(\frac{b_{fc}}{b_{fc} + P_{co}} \right)^2 k_{fh} P_h \qquad [10]$$

This equation reduces to the current density for dissociative chemisorption of hydrogen in the limiting case where P_{co} is 0, as one would expect. j_{ll} only gets small when P_{co} becomes much larger than the CO desorption-adsorption rate ratio.

Figures 5 and 6 show the effects of increasing k_{fh}, the rate of dissociative chemisorption of hydrogen, and k_{eh}, the rate of hydrogen oxidation, on the limiting current obtained in the presence of 100 ppm CO for the case of no electrochemical stripping of CO. This shows that k_{fh} indeed affects the limiting current but that k_{eh} only affects the current below the limiting current in the absence of CO stripping. Thus, the dissociative chemisorption step is overall the rate limiting step on a CO covered surface, as might be expected.

Figure 7 shows the CO coverage for two values of b_{fc} (with other parameters set to the base case values) as a function of η. The increase of θ_{co} with increasing overpotential at low overpotential occurs because the hydrogen coverage decreases over this range, as shown in Fig. 8.

Returning to the question of the effect of electrochemical stripping of CO on the performance of the cell, we show in Figures 9 and 10 simulated current-voltage curves for CO stripping (Figure 9) and overall cell performance (Figure 10) with increasing electrochemical rates of stripping of CO (other parameters are those of the base case) for the case of exposure to 200 ppm CO. It is evident from these curves that quite low CO stripping current densities, on the order of a few microamps/cm^2, can translate into quite large cell current densities. For example, for the case of $k_{ec} = 2 \times 10^{-7}$ with 200 mV of polarization, roughly j_{co} is 3 microamps/cm^2 and this translates into a hydrogen oxidation current density of 1 A/cm^2. This is a direct consequence of the high rate of the hydrogen oxidation process. Note, however, that there is still that a substantial penalty to be paid in terms of overpotential associated with these current densities.

Acknowledgment

We wish to acknowledge the support of the US DOE Office of Transportation Technology for their support of this work.

References

1. H. A. Gasteiger, N. M. Markovic and P. N. Ross, *J. Phys Chem.,* **99**, 8290 (1995).

2. H. A. Gasteiger, N. M. Markovic and P. N. Ross, *J. Phys Chem.*, **99,** 16757 (1995).

3. M. Iwase and S. Kawatsu, in *Proton Conducting Membrane Fuel Cells I*, S. Gottesfeld, G. Halpert and A. Landgrebe, Editors, **PV 95-23**, p12, The Electrochemical Society Proceedings Series, Pennington, NJ (1995).

4. T. A. Zawodzinski Jr., C. Karuppaiah, F. Uribe and S. Gottesfeld, *Extended Abstracts*, Electrochemical Society Fall Meeting: San Antonio, TX, October 1996: **Vol 96-2**, Abstract No. 781.

5. C. Karuppaiah, F. Uribe, T. A. Zawodzinski Jr. and S. Gottesfeld, *Extended Abstracts,* Electrochemical Society Spring Meeting: Montreal, Canada, May 1997: **Vol 97-1**

TABLE I. Base Case Parameters

Parameter	**Value**	**Unit**
b_{fc}	$2\ 10^{-5}$	–
b_{fh}	0.5	–
k_{fc}	.06	A/cm^2
k_{fh}	4.	A/cm^2
b_h	.06	V
b_c	.06	V
k_{ec}	10^{-9}	A/cm^2
k_{eh}	0.5	A/cm^2
P_h	2	atm

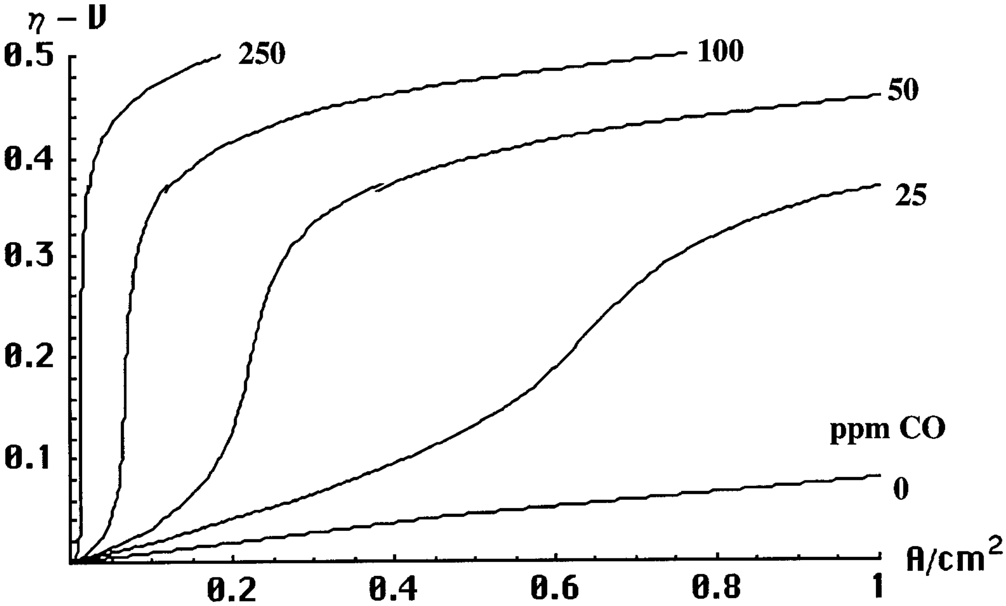

Figure 1: Anode overpotential for base case parameters in Table I as a funtion of CO concentration in the anode feed stream.

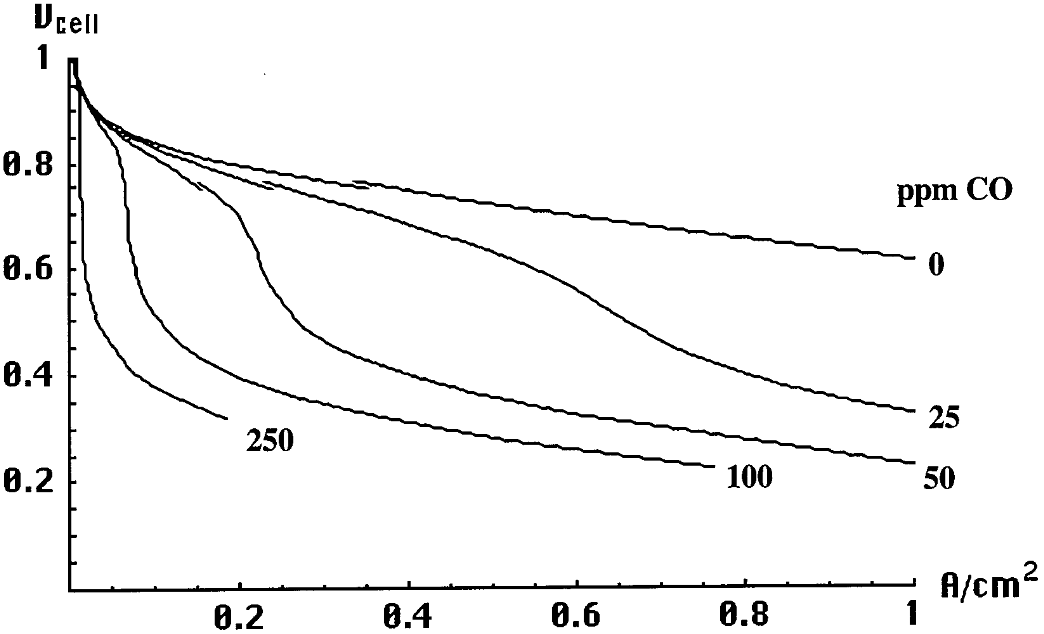

Figure 2: Cell polarization curve for base case parameters in Table I as a function of CO concentration in anode feed stream.

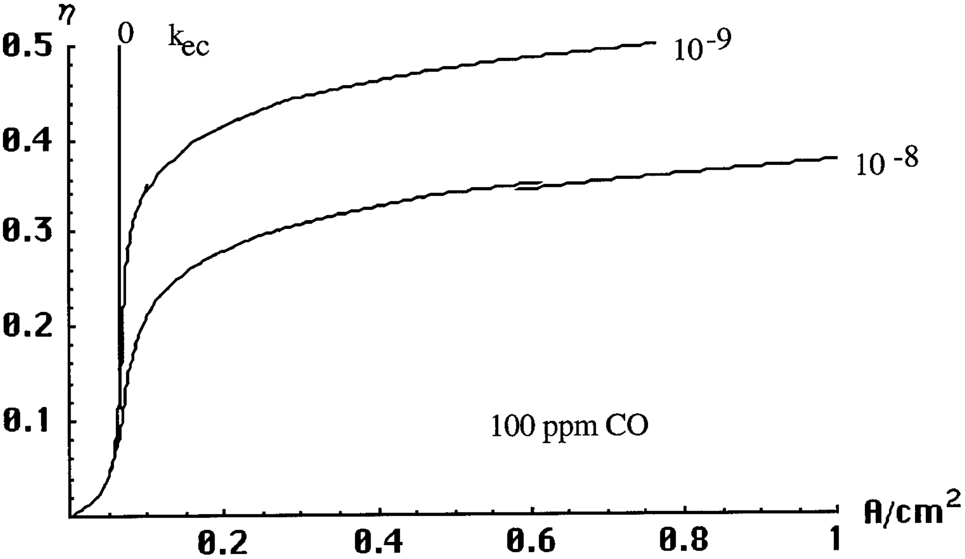

Figure 3: Anode polarization in the presence of 100 ppm CO with low values of k_{ec} to illustrate effect of low extents of CO stripping. Parameters other then k_{ec} are as the base case.

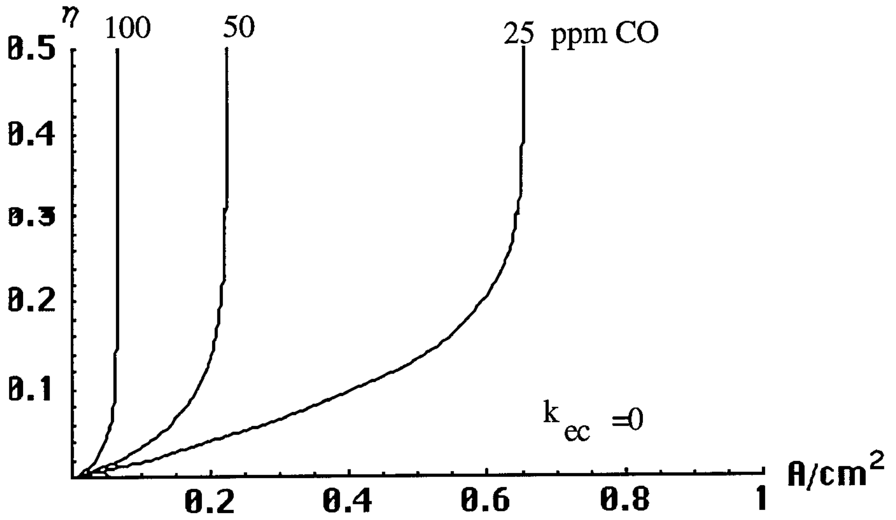

Figure 4: Effect of P_{CO} on anode polarization for no electrochemical CO stripping (k_{ec} = 0) and base case otherwise.

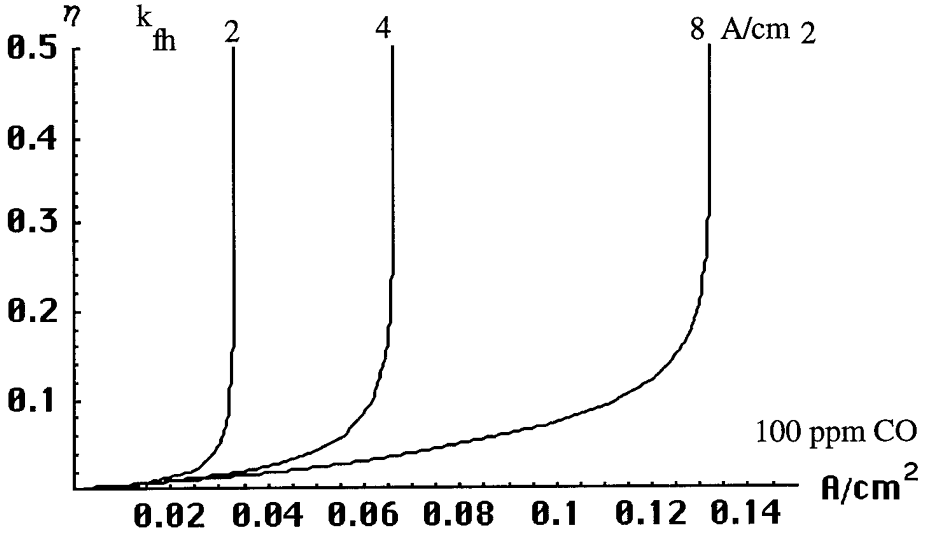

Figure 5: Effect of the rate of dissociative chemisorption of hydrogen on anode polarization for no electrochemical CO stripping (k_{ec} = 0) and base case otherwise

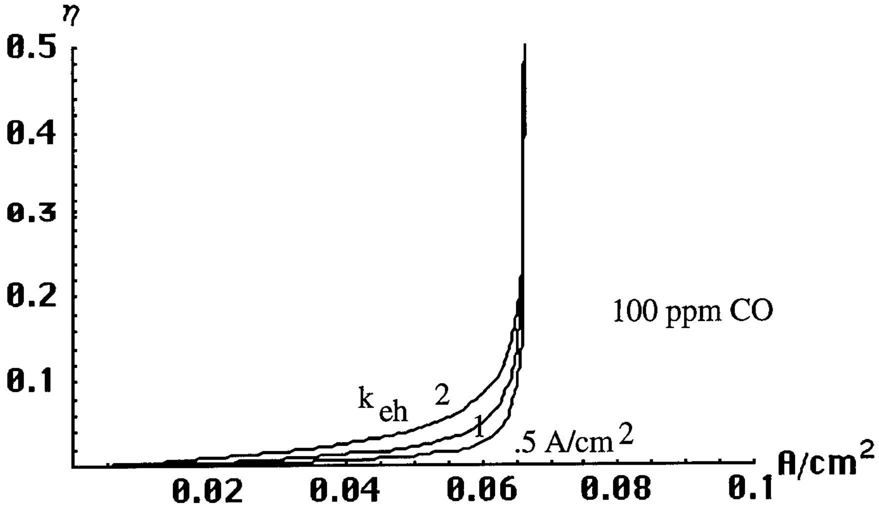

Figure 6: Effect of the rate of hydrogen oxidation on anode polarization for no electrochemical CO stripping ($k_{ec} = 0$) and base case otherwise

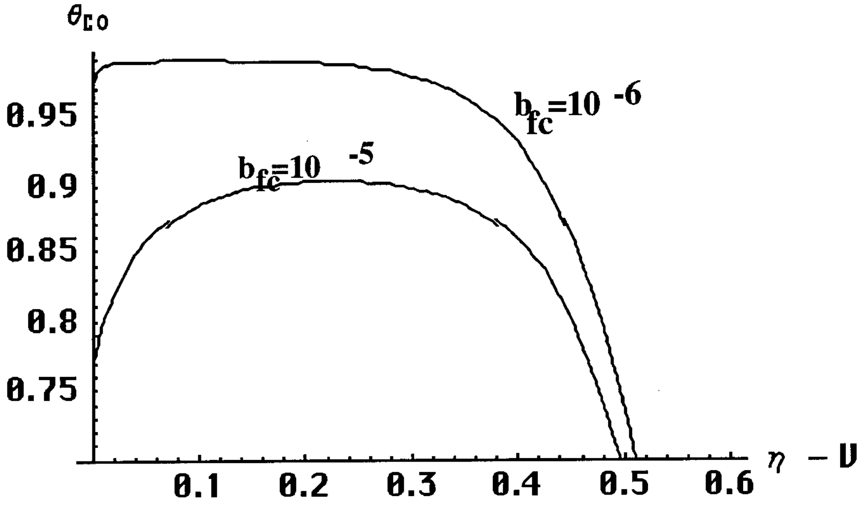

Figure 7: Calculated CO coverage as a function of anode overpotential for two different CO adsorption/desorption rate ratios (equilibrium constants); other parameters as for base case.

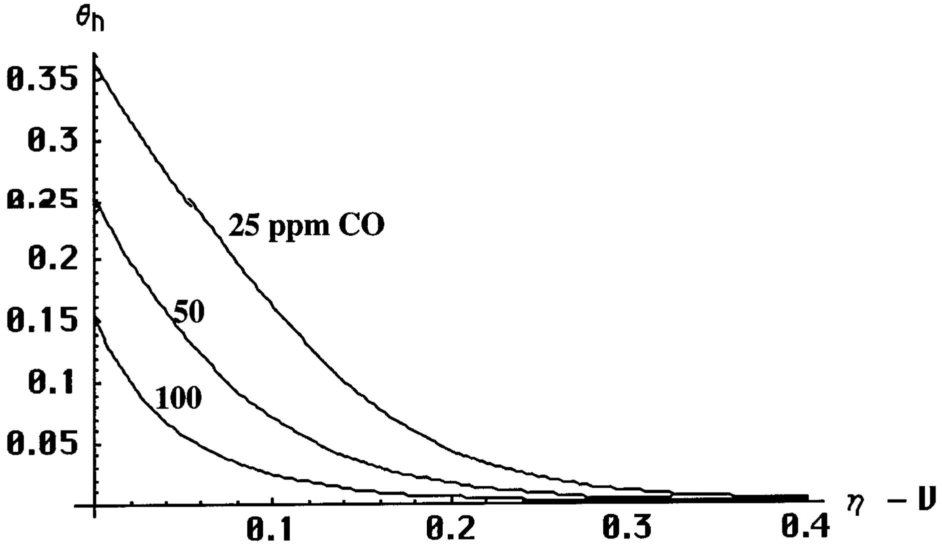

Figure 8: The H_2 coverage as a function of anode overpotential for various P_∞ levels in the anode feed stream; conditions as in Figure 7, $b_{fc} = 1 \times 10^{-5}$.

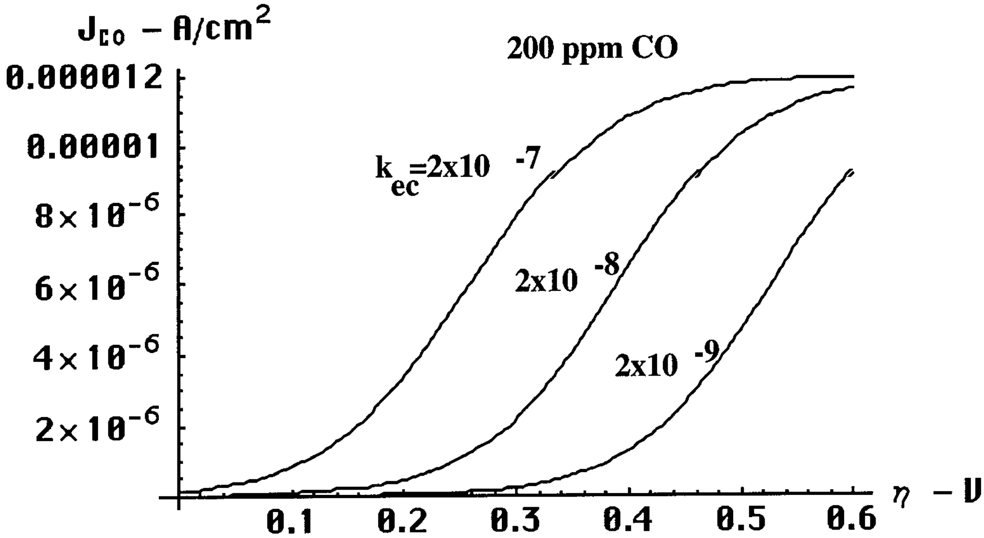

Figure 9: CO oxidation current density in the presence of 200 ppm CO as a function of potential for various values of the electrochemical rate constant for CO oxidation.

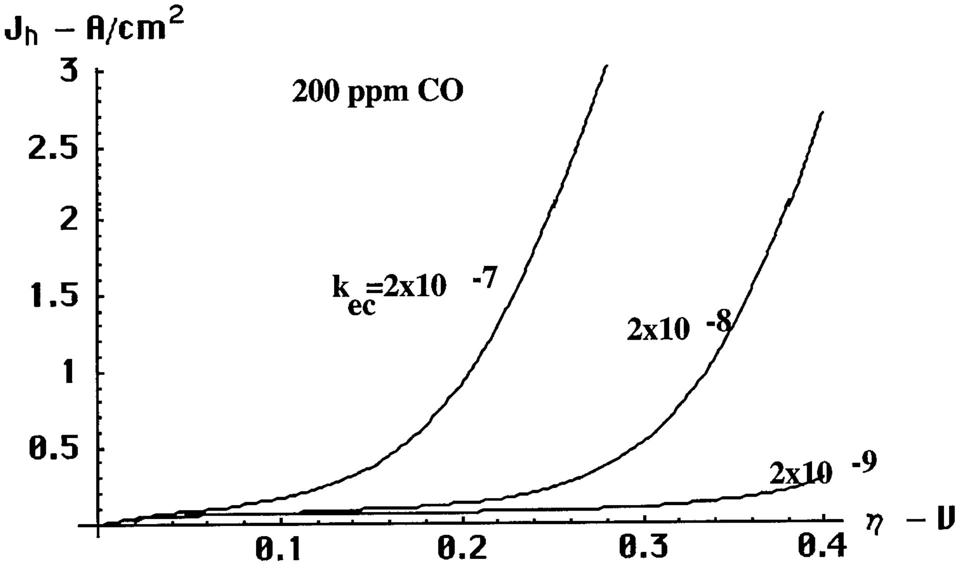

Figure 10: H_2 oxidation current density in the presence of 200 ppm CO as a function of potential for various values of the electrochemical rate constant for CO oxidation.

M97008569

Report Number (14) LA-UR--97-2196
CONF-970517--

Publ. Date (11) 199708
Sponsor Code (18) DOT, XF
UC Category (19) UC-000, DOE/ER

DOE